# V.A.7 Highly Active, Durable, and Ultra-Low PGM NSTF Thin Film ORR Catalysts and Supports

Andrew Steinbach (Primary Contact), Isaac Davy, Cemal Duru, Andrew Haug, Amy Hester, Monika Kuznia, Krzysztof Lewinski, Sean Luopa, Jason Petrin, and Grant Thoma

3M Company, Corporate Research Materials Laboratory
3M Center, Building 201-2N-19
St. Paul, MN 55144-1000
Phone: (651) 737-0103
Email: ajsteinbach2@mmm.com

DOE Manager: David Peterson
Phone: (240) 562-1747
Email: David.Peterson@ee.doe.gov

Contract Number: DE-EE0007270

Subcontractors:
- J. Erlebacher, Johns Hopkins University, Baltimore, MD
- J. Greeley and Z. Zeng, Purdue University, West LaFayette, IN
- D. Cullen, Oak Ridge National Laboratory, Oak Ridge, TN
- D. Myers and A.J. Kropf, Argonne National Laboratory, Lemont, IL

Project Start Date: January 1, 2016
Project End Date: March 31, 2019

## Overall Objectives

The overall objective is development of improved thin film oxygen reduction reaction (ORR) catalysts on nanostructured thin film (NSTF) supports for proton exchange membrane fuel cells (PEMFCs) which achieve:

- Mass activity of 0.80 A/$mg_{PGM}$ or higher.
- Platinum group metal (PGM) total content (both electrodes) of ≤0.1 g/kW at 0.70 V.
- PGM total loading (both electrodes) <0.1 $mg_{PGM}/cm^2$.
- Mass activity durability of <20% loss.
- Loss of performance <20 mV at 0.8 A/$cm^2$ and 1.5 A/$cm^2$.

## Fiscal Year (FY) 2017 Objectives

- Develop new ultra-thin film (UTF) and nanoporous thin film (NPTF) electrocatalysts, towards achievement of activity, durability, and cost objectives.
- Employ advanced composition and structural analysis to guide electrocatalyst development, including transmission electron microscopy, energy dispersive X-ray spectroscopy (EDS), and X-ray adsorption fine structure spectroscopy (XAFS).
- Validate density functional theory (DFT) and kinetic Monte Carlo (kMC) models, and utilize models to predict novel electrocatalyst concepts with improved activity and durability.
- Validate high throughput electrocatalyst fabrication and characterization methods, towards acceleration of project electrocatalyst development.

## Technical Barriers

This project addresses the following technical barriers from the Fuel Cells section of the Fuel Cell Technologies Office Multi-Year Research, Development, and Demonstration Plan.

(A) Durability

(B) Cost

(C) Performance

## Technical Targets

Table 1 summarizes 2017 project status against the relevant 2020 DOE targets and project targets. All reported status values are measurements made in 50 $cm^2$ active area membrane electrode assemblies (MEAs). PGM total content and PGM total loading are reported for two MEAs, containing either UTF PtNi or NPTF PtNiIr catalysts. MEAs were evaluated with an anode gas diffusion layer and a cathode interlayer optimized to improve NSTF MEA operational robustness [1]. The cathode interlayer contains 16 $\mu g_{Pt}/cm^2$. Both MEAs had less PGM total loading than the DOE target (0.125 mg/$cm^2$) and the UTF catalyst MEA also exceeded the DOE PGM total content target (0.125 g/kW) while simultaneously meeting the DOE Q/ΔT target of 1.45 kW/°C.

Beginning of life (BOL) mass activity values were 0.38 A/$mg_{PGM}$ and 0.44 A/$mg_{PGM}$ (vs. 0.44 A/mg target) for NPTF PtNiIr and UTF PtNiIr catalysts, respectively. A new UTF catalyst was developed which achieved mass activity of 0.56 A/$mg_{PGM}$, significantly exceeding the DOE target. After evaluation under the DOE electrocatalyst accelerated stress test (AST), both UTF and NPTF PtNiIr catalysts demonstrated a loss in catalytic (mass) activity of 45% (vs. 40% DOE target) and a loss in performance at 0.8 A/$cm^2$ of less than 25 mV (vs. DOE target of 30 mV loss).

**TABLE 1.** Status against Technical Targets

| Characteristic | 2020 Target and Units | Project Target | 2017 Status | |
|---|---|---|---|---|
| | | | UTF | NPTF |
| PGM total content (both electrodes) | 0.125 g/kW ($Q/\Delta T \leq 1.45$) | 0.1 ($Q/\Delta T = 1.41$) | 0.13[2](1.41) 0.12[2](1.45) | 0.15[1](1.41) 0.14[1](1.45) |
| PGM total loading (both electrodes) | 0.125 mg/cm$^2$ | 0.10 | 0.077[2] | 0.122[1] |
| Loss in catalytic (mass) activity | 40% | 20 | 45[4] | 45[3] |
| Loss in performance at 0.8 A/cm$^2$ | 30 mV | 20 | 23[4] | 21[3] |
| Loss in performance at 1.5 A/cm$^2$ | 30 mV | 20 | NA | NA |
| Mass activity @ 900 $mV_{iR\text{-}free}$ | 0.44 A/mg | 0.80 (in MEA) | 0.44[4] 0.56[5] | 0.38[3] |

[1]2017 (Jan.) NPTF best of class (BOC) MEA. 0.016 $mg_{Pt}$/cm$^2$ NSTF anode, 0.090 $mg_{PGM}$/cm$^2$ NPTF PtNiIr cathode, 0.016 $mg_{Pt}$/cm$^2$ cathode interlayer.
[2]2017 (Jan.) UTF BOC MEA. 0.015$mg_{Pt}$/cm$^2$ NSTF anode, 0.046 $mg_{PGM}$/cm$^2$ UTF PtNi cathode, 0.016 $mg_{Pt}$/cm$^2$ cathode interlayer.
[3]NPTF PtNiIr/NSTF cathode from 2017 (Jan.) NPTF BOC MEA, 0.09$mg_{PGM}$/cm$^2$.
BOL and/or after 30,000 electrocatalyst AST cycles.
[4]UTF PtNiIr. BOL and/or after 30,000 electrocatalyst AST cycles.
[5]UTF catalyst, 26 $\mu g_{PGM}$/cm$^2$.
PGM total content values at 90°C cell, 1.5 atmA $H_2$/air, and 0.692 V and 0.700 V cell voltages.

## FY 2017 Accomplishments

- Developed four distinct electrocatalysts which met or exceeded the DOE 2020 mass activity target of 0.44 A/$mg_{PGM}$, including one electrocatalyst with 0.56 A/$mg_{PGM}$. Electrocatalysts were evaluated in MEA format with cathode electrode loadings below those required to achieve DOE 2020 PGM total loading (both electrodes) target. Three of the electrocatalysts were based on the UTF morphology, and the highest mass activity electrocatalyst demonstrated a specific activity of 3 mA/cm$^2_{Pt}$, 2.5x higher than UTF pure Pt catalyst and 7.5x higher than pure Pt nanoparticle catalyst.
- Established quantitative relationships between fabrication processes, physical properties, and resultant catalyst performance with three UTF PtNi catalyst characteristic variables. Catalyst activity correlated with bulk Pt-Pt strain after fuel cell testing, which was influenced by the pre-test electrocatalyst composition, grain size, and electrocatalyst film thickness. Through this work, an optimized UTF PtNi catalyst was developed and achieved PGM total content of 0.12 g/kW, exceeding the DOE target of ≤0.125 g/kW, and PGM total loading (both electrodes) of 0.077 $mg_{PGM}$/cm$^2$, exceeding the DOE target of ≤0.125 $mg_{PGM}$/cm$^2$.
- Electrocatalyst models were successfully validated against the experiment. The kMC model was validated for predictive capability towards nanoporosity formation, specific area development, and compositional evolution of NPTF $Pt_xNi_{1-x}$. Model predictions agreed with experiment, both in terms of compositional sensitivity and relative magnitude of nanoporosity development for catalysts with seven initial Pt mole fractions. The DFT modeling of activity and stress predictions of Pt skins (various thicknesses, pseudomorphic and strain-relaxed) on $Pt_xNi_{1-x}$ bulk films has been completed. Model predictions of activity variation with Pt-Pt bond distances agree in trend with experiment. Validated DFT and kMC models are now used to predict new electrocatalyst candidates with improved activity and durability.
- Developed new UTF and NPTF catalysts based on PtNi with Ir-modified surfaces, leading to improved activity, durability, and/or performance. We identified that addition of Ir to UTF Pt and PtNi surfaces can result up to a 46% increase in PGM mass activity over Ir-free catalysts. Optimal NPTF PtNiIr achieved 0.38 A/$mg_{PGM}$ (vs. 0.44 A/$mg_{PGM}$ target), durability of 45% mass activity loss (vs. 40% loss target) and 21 mV loss at 0.8A/cm$^2$ (vs. 30 mV loss target), and specific power of 7.3 kW/g (vs. 8.0 kW/g target). The to-date optimal UTF PtNiIr catalyst met the DOE mass activity target and exceeded the loss in performance at 0.80 A/cm$^2$ durability target and achieved 45% mass activity loss, which approached the 40% loss target.
- Modeling and advanced characterization were utilized to determine the role of Ir towards the observed activity and durability enhancement imparted by the addition of Ir to the surface of NPTF and UTF PtNi. Transmission electron microscopy and EDS analyses indicated that Ir increased Ni retention in NPTF PtNi after accelerated durability testing, and Ir content was stable. XAFS analysis indicates that surface Ir is generally minimally coordinated with other elements, but may reduce formation of Ni oxide. DFT modeling indicated that it is energetically favorable for Ir to move below the Pt surface, enabling ORR activity on the exposed Pt. kMC

modeling was utilized to evaluate the evolution and stability of nanoporosity in NPTF PtNi with a Ir surface layer, and determined that Ir preferentially forms a shell over the nanoporous PtNi structure which keeps the porous structure from coarsening and collapsing onto itself via capillary wetting.

- Progress was made towards validation and implementation of high throughput (HT) electrocatalyst development methods. This year, HT XAFS characterization has been developed and validated, successfully characterizing the atomic scale structure of NSTF catalysts with gradient composition with spatial position. Additionally, HT electrochemical characterization of catalyst activity and surface area has been established as reproducible.

✧ ✧ ✧ ✧ ✧

## INTRODUCTION

State-of-the-art membrane electrode assemblies utilized in today's prototype automotive traction fuel cell systems continue to suffer from key technical and economical limitations of high cost, insufficient durability, and low robustness to off-nominal operating conditions. Many state-of-the art MEAs based on conventional carbon-supported Pt nanoparticle catalysts currently incorporate precious metal loadings which are significantly above those needed to achieve MEA cost targets. As electrode catalyst loading is lowered to reduce cost, performance and durability typically decrease significantly. New catalysts and electrodes are needed which simultaneously achieve the cost, performance, and durability targets to enable the possibility of wide-spread commercialization of automotive fuel cells.

This project focuses on development of novel thin-film electrocatalysts based on 3M's NSTF catalyst technology platform. NSTF electrocatalysts and electrodes are a unique approach towards addressing key technical commercialization challenges. The thin film electrocatalyst structure imparts substantially high ORR specific activities and high resistance to electrocatalyst dissolution and sintering induced by electrochemical cycling [2]. The NSTF support is based on an oriented, sub-micron scale crystalline organic pigment whisker, not carbon particles, which enables exceptional resistance to corrosion in fuel cell and water electrolysis applications [3]. Traditional NSTF electrodes, which are a single layer of NSTF electrocatalyst particles partially embedded into an ion-conducting membrane, are ultrathin (<1 μm) and do not require ionomer for proton conduction [4]. When integrated into state-of-the-art operationally robust MEAs, the NSTF electrode structure enables high absolute and specific power densities [1].

## APPROACH

The project approach is to establish relationships between electrocatalyst functional response (activity, durability), physical properties (bulk and surface structure and composition), and fabrication processes (deposition, annealing, dealloying) via systematic investigation. Once established, these relationships will be utilized towards development of electrocatalysts with further improved properties. Electrocatalysts will be generated in one of two distinct morphologies, nanoporous thin film and ultrathin film, each with distinct pathways towards achieving project targets. Additionally, this project utilizes high throughput material fabrication and characterization, electrocatalyst modeling, and advanced physical characterization to guide and accelerate development.

## RESULTS

We previously reported initial results from a new UTF PtNi electrocatalyst system, with systematic studies of the impacts of composition and structure on activity and performance [5]. Mass activity was found to depend strongly on annealing conditions, ranging from 0.15 A/mg (unannealed) to as high as 0.39 A/$mg_{PGM.}$ Additional analysis was conducted this year towards understanding the underlying causes of the activity sensitivity towards annealing. UTF PtNi catalysts with 0.027 mg/$cm^2$ were prepared and characterized with a range of annealing times at either one of two annealing temperatures (T1 < T2), summarized in Figure 1.

Specific activity generally increased as annealing time and temperature decreased through the process condition ranges evaluated (Figure 1A). After fuel cell testing, some of the electrocatalysts were analyzed for composition by EDS, and the bulk Pt-Pt strain of the catalyst, relative to bulk pure Pt, was calculated based on the measured composition and Vegard's law. Figure 1B shows that as the annealing time and temperature increased, the calculated bulk strain increased, and the trends in bulk strain were qualitatively similar to the observed variation in specific activity from Figure 1A. Figure 1C directly compares the relationship between the calculated bulk strain and the catalyst specific activity, and a very good correlation is observed over nearly a 2.5x range of specific activity. Figure 1D summarizes DFT model predictions of catalyst activity for pseudomorphic Pt skins of various thicknesses on $Pt_xNi_{1-x}$ substrates of varying strain (composition). The DFT model predicts a peak in activity near 2.5% strain for Pt skins between 2–4 monolayers, and the peak activity is approximately 20x higher than unstrained Pt(111). The DFT prediction of activity vs. strain agrees well with the experimental data in trend but not in magnitude. The cause for the discrepancy in magnitude between model and experiment is not known and is currently under investigation.

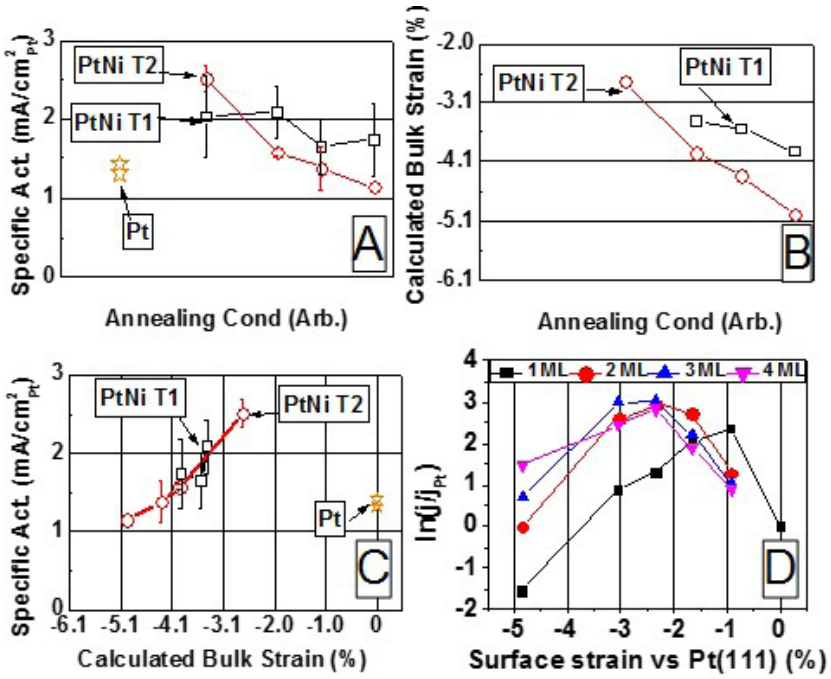


Act. – activity; Arb. – arbitrary

**FIGURE 1.** UTF PtNi activity dependence on bulk and surface strain. (A) Activity vs. annealing conditions. (B) Calculated bulk strain vs. annealing conditions. (C) Correlation of specific activity to calculated bulk strain. (D) DFT model prediction of activity vs. strain (note logarithmic scale).

Based on the understanding developed with the UTF PtNi system and previous studies with NPTF PtNi, development expanded into the fabrication and characterization of several new alloy candidates. Five new Pt binary alloy candidate systems were fabricated and characterized in MEA for beginning of life activity and $H_2$/air performance. Each alloy system was evaluated with a range of Pt mole fractions and annealing conditions and one of two Pt loadings (25–30 $\mu g_{Pt}/cm^2$ for UTF catalysts, 80–90 $\mu g_{Pt}/cm^2$ for NPTF catalysts). Additionally, NPTF catalysts were dealloyed prior to MEA fabrication to minimize leachable alloying element content and potentially inducing nanoporosity. Figure 2 summarizes the mass activities and $H_2$/air performances from the highest performing UTF and NPTF catalysts identified in each binary alloy system (PtNi and new alloys "B," "C," "D," "E," and "F"). Additionally, data for NSTF Pt catalyst and Pt nanoparticle catalysts on Vulcan carbon (Pt/V) in dispersed electrodes is included for reference. Figures 2A and 2B summarize BOL mass activity for the NPTF and UTF alloys, respectively. Four catalysts overall were identified with mass activity of 0.39 $A/mg_{PGM}$ or higher, NPTF PtNi, UTF PtNi, UTF B and UTF E. The highest overall activity of 0.47 $A/mg_{PGM}$ was obtained with NPTF PtNi, which exceeded the DOE target of 0.44 $A/mg_{PGM}$. Figures 2C and 2D summarize the $H_2$/air performances obtained at 1.5 atmA $H_2$/air reactant pressures for the NPTF and UTF catalysts, respectively. For NPTF catalysts, PtNi, B, C, and F had improved performance at high current density over Pt/V electrodes with 0.10 $mg_{Pt}/cm^2$ electrode loading. The best overall high current density performance was obtained with NPTF "F," which yielded a ca. 100 mV improvement over Pt/V at 1.0 $A/cm^2$ current density. UTF PtNi, B, D, and F catalysts with 25–30 $\mu g_{Pt}/cm^2$ had higher $H_2$/air performance than the reference Pt/V catalyst containing 50 $\mu g_{Pt}/cm^2$ electrode loading. UTF PtNi and F yielded the highest overall high current density performance, as much as 69 mV higher than Pt/V at 0.50 $A/cm^2$ current density.

Several electrocatalyst candidates were also evaluated for durability with the DOE electrocatalyst AST [6], consisting of 30,000 triangle wave cycles between 0.60 V and 1.0 V at 50 mV/s. Last year, we reported that the integration of an additive substantially improved the durability of NPTF PtNi catalyst. Mass activity losses decreased from about 65–70% without the additive to 42% with the additive, close to the DOE target of 40%. While effective at improving the durability, BOL mass activity and $H_2$/air performance were suppressed relative to additive-free NPTF PtNi catalysts [5]. This year, new electrocatalyst development was conducted towards improving the mass activity, performance, and durability of NPTF PtNi and UTF PtNi via integration of small amounts of Ir. Figure 3A summarizes beginning of life mass activity of NPTF PtNiIr catalysts as a function

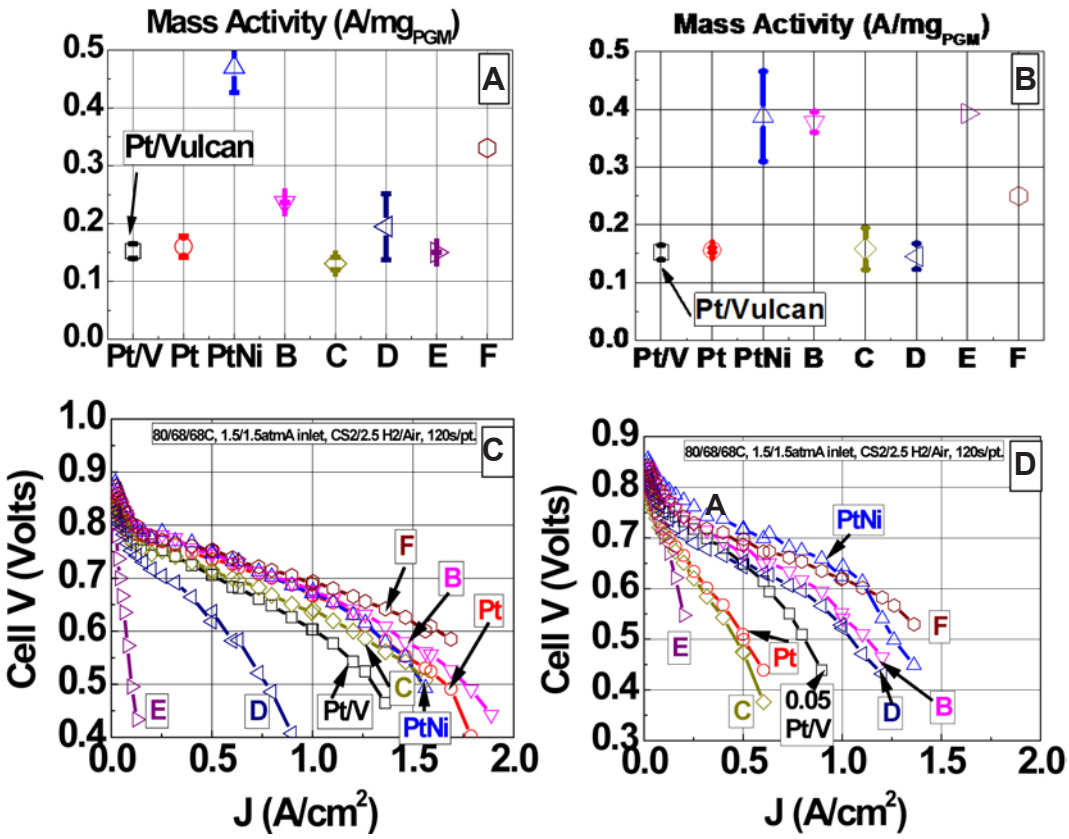


**FIGURE 2.** Mass activity and $H_2$/Air performance of Pt on Vulcan, Pt/NSTF, PtNi/NSTF, and NSTF Pt binary alloys "B," "C," "D," "E," and "F." (A) NPTF catalyst mass activity. (B) UTF catalyst mass activity. (C) NPTF catalyst $H_2$/Air performance at 80°C, 1.5 atmA $H_2$/air. (D) UTF catalyst $H_2$/air performance.

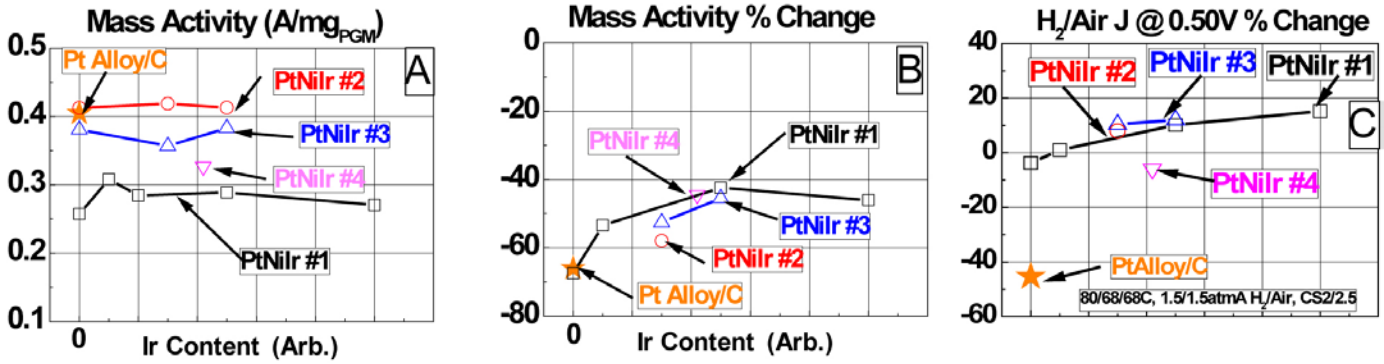


**FIGURE 3.** Mass activity and durability of several NPTF PtNiIr catalysts as a function of Ir content. (A) Mass activity at beginning of life. (B) Change in mass activity after accelerated durability testing. (C) Change in $H_2$/air current density at 0.50 V cell voltage after durability testing.

of Ir content and Ir integration method (#1, #2, #3, and #4). Reference data for a high activity Pt alloy nanoparticle on carbon catalyst with an electrode loading of 0.09 $mg_{PGM}/cm^2$ is included for reference. The mass activity of NPTF PtNiIr varied from ca. 0.25 A/$mg_{PGM}$ to 0.41 A/$mg_{PGM}$ and depended primarily on Ir integration method, not on Ir content through the range evaluated. Figure 3B shows that with integration method #1 and #3, mass activity losses after accelerated durability testing were as low as 42% and 45%, respectively, and appeared to decrease as Ir content increased to a relatively moderate level. Figure 3C summarizes the changes in $H_2$/air current density at 0.50 V cell voltage after the durability testing, and for most NPTF PtNiIr catalysts the performance at 0.50 V was either unchanged or slightly

improved after the test. With PtNiIr#1, performance improvement after the durability test appeared to increase monotonically with Ir content. For reference, the Pt alloy on carbon catalyst lost 70% mass activity and 50% of the $H_2$/air current density at 0.50 V after the durability test.

Ir integration studies were also conducted with UTF Pt and PtNi to determine the impact of Ir on activity, performance, and durability. Figure 4A summarizes beginning of life mass activities for UTF PtIr and three UTF PtNiIr catalysts as a function of Ir content. The PtIr catalyst contained 30 $\mu g_{Pt}/cm^2$ loading in the electrode and the three PtNiIr catalysts' loadings were 9 $\mu g_{Pt}/cm^2$, 26 $\mu g_{Pt}/cm^2$, and 50 $\mu g_{Pt}/cm^2$, respectively. The PGM mass activity of all four catalysts depended strongly on Ir content, with evidence of an activity peak through a narrow Ir content range which may be specific to each catalyst. Peak PtIr mass activity was 45% higher than comparable Ir-free Pt, and peak PtNiIr #1 activity was 46% higher than comparable Ir-free PtNi #1. Peak mass activities for the 9 $\mu g_{Pt}/cm^2$, 26 $\mu g_{Pt}/cm^2$, and 50 $ug_{Pt}/cm^2$ UTF PtNi catalysts were 0.36 $A/mg_{PGM}$, 0.41 $A/mg_{PGM}$, and 0.44 $A/mg_{PGM}$. The increased mass activity observed within the narrow and low Ir content range was primarily due to increased specific activity. Figure 4B shows that mass activity losses of the PtIr and PtNiIr after accelerated durability ranged from 35% to 65% vs. the 40% DOE target. The UTF PtNiIr catalyst with the highest beginning of life mass activity of 0.44 $A/mg_{PGM}$ lost 45% mass activity after accelerated durability testing, which exceeded the project go/no-go criteria for Budget Period 1. The data suggests that the mass activity durability of the highest activity PtNiIr catalysts with optimal Ir content is comparable to or lower than Ir-free catalyst, but at higher Ir contents the mass activity durability may be moderately improved over Ir-free. While the impact of Ir on mass activity durability of UTF Pt and PtNi was moderate, Ir did significantly improve the durability of specific surface area and $H_2$/air performance at high current density. Figure 4C shows that the specific area losses after the accelerated durability test decreased monotonically with increasing Ir content for all four Ir-containing catalysts. Figure 4D shows that the loss in $H_2$/air current density at 0.50 V cell voltage also generally improved with increasing Ir content for the UTF PtIr and the two higher Pt content PtNiIr catalysts. With the highest Pt-content UTF PtNiIr catalyst, performance change at 0.50 V ranged from essentially no change to a modest improvement, and loss in performance at 0.80 V was 21 mV, exceeding the DOE target of 30 mV loss.

Modeling and advanced characterization were utilized to determine the role of surface Ir towards the observed activity and durability enhancements with NPTF and UTF PtNiIr catalysts. Catalysts were evaluated for atomic-scale structure by scanning transmission electron microscopy (STEM) imaging and for bulk composition by EDS. Figure 5 summarizes the analysis of a particular UTF PtNiIr catalyst, evaluated after fuel cell conditioning. Ir content was relatively stable through fuel cell conditioning and after the electrocatalyst AST, and Ir deposited on the catalyst surface largely remains at the surface. DFT modeling was conducted

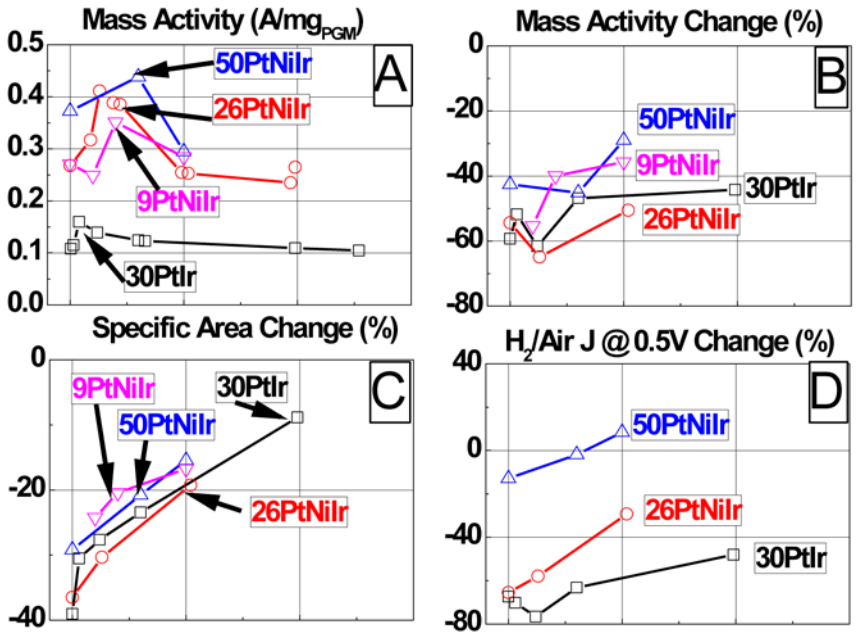


**FIGURE 4.** Mass activity and durability as a function of Ir content for UTF PtIr and three PtNiIr catalysts with electrode Pt loadings ranging from 9 $\mu g/cm^2$ to 50 $\mu g/cm^2$. (A) PGM mass activity at beginning of life. (B–D) Changes in PGM mass activity, PGM specific area, and current density at 0.50 V after the DOE electrocatalyst AST.

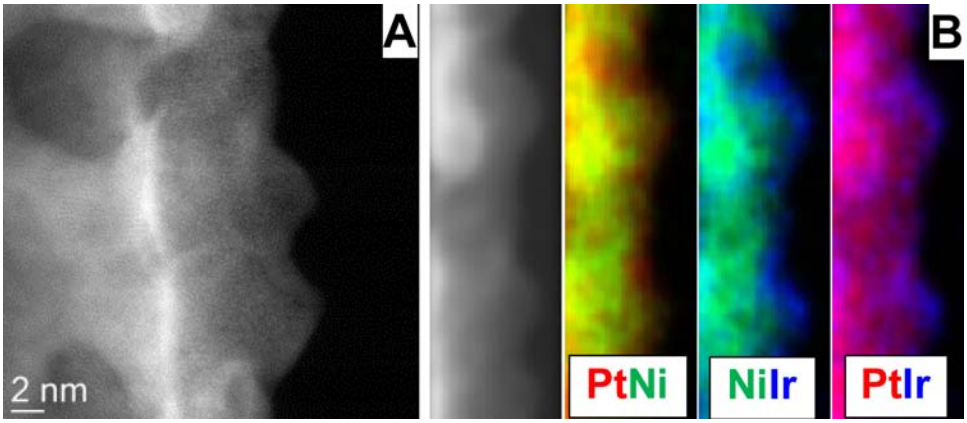


**FIGURE 5.** STEM-EDS analysis of UTF PtNiIr catalysts. (A) High-angle annular dark field STEM. (B) EDS composition maps.

to assess the thermodynamic stability of Ir-modified Pt(332) surfaces with varying surface coverages of Ir (Figure 6). The model determined that the formation energy for Ir deposition on the surface of Pt(332) is not energetically favorable, and that this formation energy is significantly reduced upon surface rearrangement where Ir is covered by a monolayer of Pt. kMC modeling was conducted to assess the impact of surface Ir content on the nanoporosity formation in PtNi. The model appeared to accurately capture the nanoporous structure obtained experimentally, as shown in Figure 7. The kMC model predicted that Ir deposited on the surface is relatively immobile with potential cycling, consistent with experimental observations. Additionally, the model suggests that Ir may enhance the nanoporous surface area durability via promotion of capillary wetting of Pt and Ni onto the stable Ir shell.

In additional catalyst development work, two new UTF Ir-free catalysts have been identified with further improved mass and specific activities over UTF PtNi (Figure 8). Average mass activities for the two new catalysts were 0.47 A/$mg_{PGM}$ and 0.56 A/$mg_{PGM}$ as measured in MEA, both exceeding the DOE 2020 target of 0.44 A/$mg_{PGM}$. The new catalysts have markedly higher specific activity than UTF Pt and PtNi, as much as 50% higher than UTF PtNi, 2.5x higher than UTF Pt, and 7.5x higher than Pt nanoparticle catalyst.

Select NPTF PtNiIr, UTF PtNi, and UTF PtNiIr catalysts from above were evaluated for rated and specific power density. The catalysts were integrated into MEAs with previously-identified components which enable improved operational robustness of NSTF MEAs, including an optimized anode gas diffusion layer and cathode interlayer, which contains 16 $\mu g_{Pt}/cm^2$ [1]. Figure 9 summarizes the measured $H_2$/air polarization curves for the three 2017 catalysts, as compared to the pre-project baseline. Polarization curves were obtained with 90°C cell temperature and 1.5 atmA $H_2$/air reactant pressures, conditions relevant for assessment of rated and specific power densities at the DOE MEA Q/ΔT heat rejection target of 1.45 kW/°C. Status against relevant DOE targets is summarized in Table 2. The absolute performance of the 2017 NPTF PtNiIr catalyst overlaps the performance obtained with the baseline NPTF PtNi (no Ir) catalyst. Overall catalyst loading of the 2017

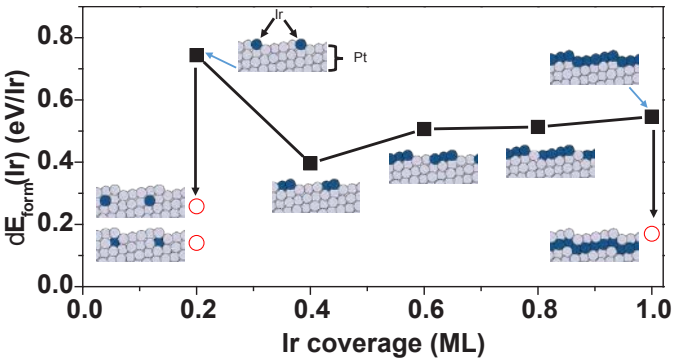


**FIGURE 6.** DFT predicted formation energies of Ir-modified Pt(332) surfaces.

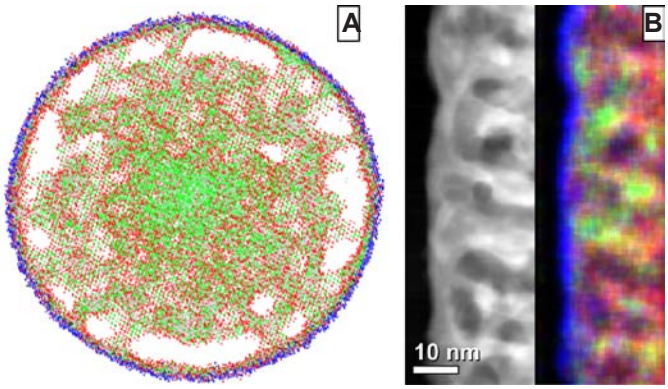


**FIGURE 7.** Structure of modeled and experimental dealloyed NPTF PtNiIr. (A) kMC model. (B) STEM-EDS analysis.

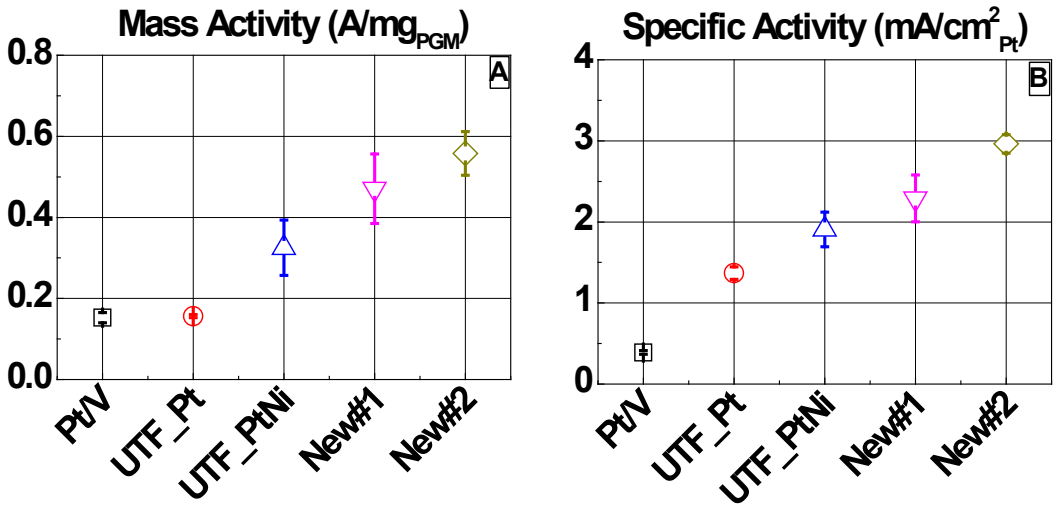


**FIGURE 8.** Mass activity of UTF Pt, PtNi, and new catalysts.

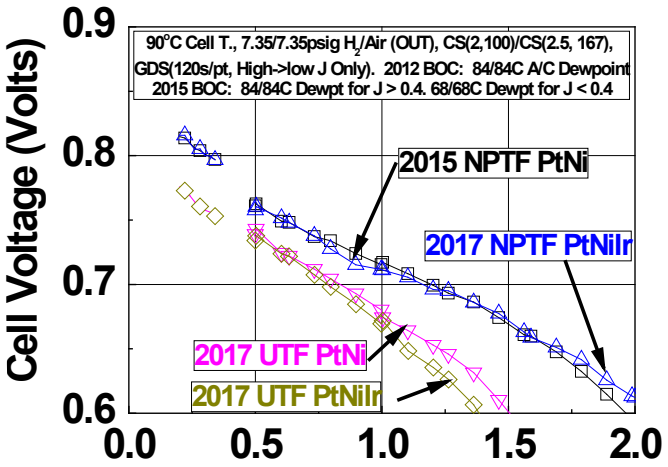


GDS – galvanodynamic scan

**FIGURE 9.** Performance of UTF and NPTF PtNi and PtNiIr catalysts.

NPTF PtNiIr MEA was reduced slightly vs. baseline to just below the DOE target, yielding modestly improved specific power which was 91% of the DOE target. Both the 2015 and 2017 MEAs slightly exceeded the DOE ¼ power target of 0.30 A/cm$^2$ at 0.80 V. Along with the improved MEA loading and specific power density, the 2017 NPTF PtNiIr cathode has improved mass activity durability vs. the baseline (45% vs. 65% loss for the NSTF cathode) and exceeded the DOE performance loss at 0.8 A/cm$^2$ target. The UTF PtNi and PtNiIr MEAs' absolute performances were substantially lower than those obtained with the NPTF PtNi and PtNiIr MEAs. Rated power densities of the UTF PtNi and PtNiIr MEAs were 0.63 W/cm$^2$ and 0.58 W/cm$^2$, respectively, which are substantially below the DOE target of 1 W/cm$^2$. The primary reason for the relatively lower absolute performance of the UTF MEAs than the comparative NPTF MEAs is because the UTF catalysts had ca. 50% lower absolute PGM loading in the NSTF cathode electrodes. The UTF PtNi MEA achieved the DOE specific power target of 8.1 kW/$g_{PGM}$ while meeting the DOE Q/ΔT heat rejection target, and had 38% lower PGM total loading (both electrodes) than the DOE target. The UTF PtNiIr MEA absolute power density was slightly lower than the UTF PtNi MEA, but met the total loading and performance loss at 0.8 A/cm$^2$ targets.

Work has continued towards establishment of reproducible methods for HT electrocatalyst development. Last year, we reported that we had developed a method of fabricating $Pt_xNi_{1-x}$ catalyst with a range of spatially-varying compositions, and that spatial variation in the catalyst's composition and bulk crystalline structure could be reproducibly characterized via HT-compatible methodologies. This year, we have validated a method for conducting HT XAFS towards characterizing the atomic scale catalyst structure with two gradient composition $Pt_xNi_{1-x}$ catalysts. Full spectral analysis and fitting conducted on Pt-rich and Ni-rich ends of the gradient catalyst substrates showed excellent reproducibility of coordination numbers and bond lengths within the three annealed and unannealed sets. The spectra of intermediate compositions were determined via linear combinations of the Pt-rich and Ni-rich endpoint spectra, allowing rapid extraction of the atomic structure information at intermediate compositions. An example of this analysis is shown in Figure 10A, which shows the Pt-Pt, Pt-Ni, and Ni-Ni bond distances determined from a gradient composition PtNi catalyst. Additionally, work has continued towards establishment of reproducible electrochemical characterization of HT-fabricated catalysts with a segmented cell. Reproducibility of catalyst activity has been established with a homogenous catalyst, yielding a 3.2% relative standard deviation across three separate replicate MEA measurements and across all 121 individual segments, exceeding the project

**TABLE 2.** Best of Class MEAs Loading, Specific Power, Rated Power, and ¼ Power Performances

| MEA Construction | Total MEA Loading (mg/cm$^2$) | Spec. Power @ Q/ΔT =1.45 (kW/g$_{PGM}$) | Rated Power @ Q/ΔT=1.45 (W/cm$^2$) | 1/4 Power J @ 0.80V (A/cm$^2$) | Electrocatalyst AST Durability (NSTF catalyst only) | |
|---|---|---|---|---|---|---|
| | | | | | Mass Act. Loss (%) | Loss @ 0.8A/cm$^2$ (mV) |
| DOE 2020 Target | 0.125 | 8.0 | 1.000 | 0.300 | 40 | 30 |
| Baseline 2015 NPTF PtNi | 0.131 | 6.8 | 0.891 | 0.310 | ~65 | NA |
| 2017 NPTF PtNiIr | 0.122 | 7.3 | 0.897 | 0.308 | 45 | 21 |
| 2017 UTF PtNi | 0.077 | 8.1 | 0.626 | NA | 43 | 50 |
| 2017 UTF PtNiIr | ≤0.089 | ≥6.6 | 0.584 | <0.200 | 45 | 23 |

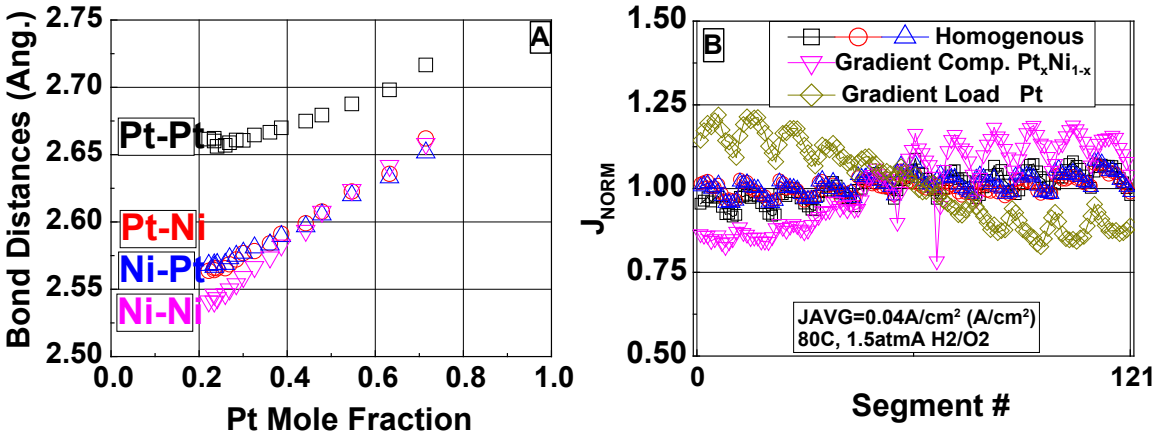


**FIGURE 10.** High Throughput Electrocatalyst Method Development. (A) HT XAFS of gradient composition PtNi catalyst. (B) HT-segmented fuel cell characterization of catalyst activity.

milestone of less than 20% relative standard deviation (Figure 10B). Two electrocatalysts with spatially-varying activity were assessed, where the activity variation was due to either a spatial variation in catalyst loading or catalyst composition. Significant spatial variations in activity were observed, consistent with expectation. However, the magnitude of activity variation appeared to be limited to a factor of 1.5 vs. the expected 2.5x and 3–4x variations for the gradient loading and gradient composition catalysts, respectively. The root-cause of this sensitivity limitation has been identified and the necessary hardware modification to resolve it is being planned.

## CONCLUSIONS AND UPCOMING ACTIVITIES

Over the past year, UTF catalysts with ultra-low PGM content have been demonstrated which meet or exceed the DOE 2020 catalyst targets for mass activity, PGM total content, PGM total loading, loss in performance at 0.8 A/cm$^2$, and the MEA Q/ΔT heat rejection target. Three compositionally-distinct UTF catalysts have met or achieved the mass activity target, with one exceeding the target of 0.44A/mg$_{PGM}$ by 27% due to an enhanced specific activity of 3 mA/cm$^2_{Pt}$. A UTF PtNi catalyst has met the platinum group metal total content (both electrodes) target of 0.125 g/kW and the DOE heat rejection Q/ΔT target of 1.45 kW/°C, with a PGM total loading (both electrodes) of 0.077 mg$_{PGM}$/cm$^2$, 40% below the target loading level. A UTF PtNiIr catalyst has exceeded the loss in performance at 0.8 A/cm$^2$ target after the electrocatalyst AST, and nearly achieves the loss in catalytic (mass) activity target. While active and durable, UTF catalyst rated power is only ca. 60% of the DOE target of 1 W/cm$^2$, due in part to the ultra-low PGM areal loadings used with current UTF catalysts. Paths to improve the rated power of UTF catalyst MEAs have been identified.

Systematic studies have revealed that the activity of UTF PtNi catalysts correlates with the catalyst Pt-Pt bulk strain after fuel cell conditioning, measured both directly (Pt-Pt bond distances via XAFS) and indirectly (composition via EDS). The post-test composition systematically depends upon the as-fabricated catalyst composition and also the catalyst grain size, which is determined by fabrication conditions. DFT modeling of monolayer-scale Pt skins on Pt$_x$Ni$_{1-x}$ alloys confirmed the catalyst activity dependence on bulk composition and agreed well with experiment in terms of the activity trends with composition. However, the model predicted activity enhancement with optimal strain

exceeded the experimentally-observed activity enhancement by a factor of 20. The causes for the discrepancy are under investigation, but may be due to non-optimal skin structures on highly-strained substrates.

Extensive studies have been conducted towards improving the durability of project electrocatalysts. One promising approach investigated was incorporation of relatively small amounts of Ir onto the surface of PtNi catalysts. Ir imparted stabilization against specific activity and specific area losses of NPTF and UTF PtNi catalysts, respectively, and generally resulted in improved performance retention at high current density. Additionally, addition of Ir to the surface of UTF Pt and PtNi within a narrow composition range increased the PGM mass activity by up to 46% vs. Ir-free. Microscopy characterization indicates that Ir is substantially stable, and electrocatalyst modeling has provided insight into the activity and durability mechanisms.

In future work, the project will continue development efforts towards achieving the overall project Budget Period 2 milestone, reflecting demonstration of a single catalyst which simultaneously exceeds the DOE 2020 targets for mass activity, mass activity durability, and specific power in an MEA. This will be accomplished by several development pathways occurring in parallel. Experiments and modeling efforts are already underway towards development of new UTF electrocatalysts with significantly further improved specific surface area and specific activity via Pt skin optimization. An additional modeling and experimental focus is identification of electrocatalyst compositions and structures which can achieve the aggressive project durability targets. Absolute performance and rated power of UTF electrocatalysts will be increased by integration of the high specific activity electrocatalyst onto NSTF supports with higher absolute surface area while maintaining the mass-specific activity and area. In addition, work has been initiated to evaluate down-selected catalysts for their impact on two key challenges for NSTF MEAs, rated power durability and break-in conditioning.

## FY 2017 PUBLICATIONS/PRESENTATIONS

**1.** A.J. Steinbach et al., "3M NSTF Electrocatalysts for PEM Fuel Cells and Water Electrolyzers," 20th International Symposium on Batteries, Fuel Cells, and Capacitors, Chiba, Japan, November 29, 2016. *Invited.*

**2.** J. Greeley, "First Principles Analysis of Interfacial Electrocatalysis," McKetta Department of Chemical Engineering at the University of Texas at Austin, Austin, TX, January 24, 2017.

**3.** D.A. Cullen et al, "Understanding the Origins of Activity through in situ Annealing and Dealloying of Fuel Cell Catalysts," 2017 Spring Materials Research Society Meeting, Phoenix, AZ, April 2017.

**4.** A.J. Steinbach, "Highly Active, Durable, and Ultra-low PGM NSTF Thin Film ORR Catalysts and Supports," USCAR Fuel Cell Tech Team, Detroit, MI, April 19, 2017.

**5.** J. Greeley, "Ab-initio Studies of Heterogeneous Catalysis and Electrocatalysis at Metal-Liquid Interfaces," Department of Chemical and Petroleum Engineering, University of Pittsburgh, Pittsburgh, PA, April 20, 2017.

**6.** Z. Zeng and J. Greeley, "DFT Studies of Electrochemical Oxygen Reduction Reactions on Pt Skin Alloys," 231st Meeting of the Electrochemical Society, New Orleans, LA, May 30, 2017.

**7.** A.J. Steinbach, 2017 Annual Merit Review, DOE Hydrogen and Fuel Cell Vehicles Technology Programs, Presentation FC143, Washington DC, June 2017.

**8.** A.J. Steinbach et al., "Ultrathin Film NSTF ORR Electrocatalysts for PEM Fuel Cells," *ECS Trans.,* submitted.

## REFERENCES

**1.** A.J. Steinbach, Presentation FC104, 2016 Annual Merit Review, DOE Hydrogen and Fuel Cell Vehicles Technology Programs, June 2016, Washington DC.

**2.** M.K. Debe et al., "Stop-Start and High-Current Durability Testing of Nanostructured Thin Film Catalysts for PEM Fuel Cells," *ECS Trans.* **3**(1) 835–853 (2006).

**3.** M.K. Debe et al., "Initial Performance and Durability of Ultra-Low Loaded NSTF Electrodes for PEM Electrolyzers," *J. Electrochem. Soc.* **159**(6) K165–K176 (2012).

**4.** M.K. Debe, "Tutorial on the Fundamental Characteristics and Practical Properties of Nanostructured Thin Film (NSTF) Catalysts," *J. Electrochem. Soc.* **160**(6) F522–F534 (2013).

**5.** A.J. Steinbach et al., "Highly Active, Durable, and Ultra-low PGM NSTF Thin Film ORR Catalysts and Supports," 2016 Annual Project Progress Report to DOE.

**6.** U.S. Department of Energy, Office of Energy Efficiency & Renewable Energy, "Fuel Cell Technologies Office Multi-Year Research, Development, and Demonstration Plan," retrieved April 6, 2015.